International Journal of Thermophysics, Vol. 21, No. 1, 2000

Simultaneous Measurements of the Thermal Conductivity and Thermal Diffusivity of Molten Salts with a Transient Short-Hot-Wire Method

X. Zhang[1, 2] and M. Fujii[1]

Received February 3,1999

A transient short-hot-wire technique has been successfully used to measure the thermal conductivity and thermal diffusivity of molten salts ($NaNO_3$, Li_2CO_3/K_2CO_3, and Li_2CO_3/Na_2CO_3) which are highly corrosive. This method was developed from the hot-wire technique and is based on two-dimensional numerical solutions of unsteady heat conduction from a short wire with the same length-to-diameter ratio and boundary conditions as those used in the actual experiments. In the present study, the wires are coated with a pure Al_2O_3 thin film by using a sputtering apparatus. The length and radius of the hot wire and the resistance ratio of the lead terminals and the entire probe are calibrated using water and toluene with known thermophysical properties. Using such a calibrated probe, the thermal conductivity and thermal diffusivity of molten nitrate are measured within errors of 3 and 20%, respectively. Also, the thermal conductivity of the molten carbonates can be measured within an error of 5%, although the thermal diffusivity can be measured within an error of 50%.

KEY WORDS: molten carbonates; molten nitrate; thermal conductivity; thermal diffusivity; transient short-hot-wire technique.

1. INTRODUCTION

Recently, the laser flash technique [1] has been widely used for measuring the thermal diffusivity of materials. The transient hot-wire method is still the most promising for measuring the thermal conductivity of liquids [2]. This method is, however, rather difficult to apply for electrically conducting and highly corrosive fluids, such as molten carbonates, because the long wires must all be insulated with anticorrosive and electrically nonconducting

[1] Institute of Advanced Material Study, Kyushu University, Kasuga 816-8580, Japan.
[2] To whom correspondence should be addressed.

0195-928X/00/0100-0071$18.00/0

materials [3]. These difficulties could be much reduced if we could develop a method with a much shorter wire than the conventional one. From this point of view, the authors [4, 5] developed a new method which used a hot wire as short as about 10 mm. As the first step, the temperature evolutions of a bare short wire were measured for pure water and some organic liquids, and by comparing the results with the two-dimensional numerical simulations, the thermal conductivity and thermal diffusivity of these liquids were simultaneously determined with a high accuracy.

In this paper, the numerical analysis on which the present method is based and the experimental arrangement are described for the probe coated with a pure Al_2O_3 film. The length and diameter of the wire and electrical resistance ratio of the lead terminals and the entire probe are determined by using pure water and toluene as the standard liquid samples. Through these calibrations, the thermal conductivity and thermal diffusivity of $NaNO_3$, Li_2CO_3/K_2CO_3, and Li_2CO_3/Na_2CO_3 are measured. The effect of an uncertainty of thermal diffusivity on the thermal conductivity evaluation is also discussed.

2. NUMERICAL ANALYSIS

Figure 1 shows the physical model and the coordinate system. The sample liquid is contained in a cylindrical vessel of radius r_o, and a short hot wire of radius r_i and length $2l$ is located on the center axis and is supported by a lead wire at each end. The hot wire is covered with an insulating material of thickness δ. The two-dimensional heat-conduction equations for this three-layer model are numerically solved under the

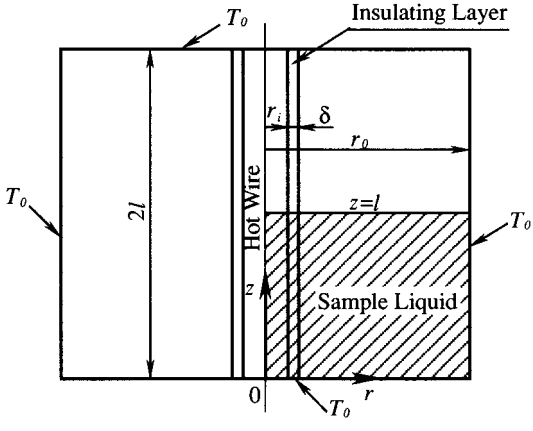

Fig. 1. Physical model and coordinate system.

following assumptions: (a) the heat generation rate per unit volume and time is uniform and constant; (b) the temperatures of the lead wires are kept at their initial temperature T_o during the heating process; and (c) the temperature distribution in the vessel is symmetric with respect to the z-axis and the plane normal to it at $z = l$. Therefore, the hatched region in Fig. 1 is taken as the solution domain.

Nondimensional basic equations are written as follows. For the hot wire,

$$\frac{\partial \theta_{sh}}{\partial \mathrm{Fo}} = \frac{1}{R_{d1}} \left(\frac{\partial^2 \theta_{sh}}{\partial R^2} + \frac{1}{R} \frac{\partial \theta_{sh}}{\partial R} + \frac{\partial^2 \theta_{sh}}{\partial Z^2} \right) + \frac{R_{c1}}{R_{d1}} \tag{1}$$

For the insulating layer and liquid layer,

$$\frac{\partial \theta_{si}}{\partial \mathrm{Fo}} = \frac{1}{R_{d2}} \left(\frac{\partial^2 \theta_{si}}{\partial R^2} + \frac{1}{R} \frac{\partial \theta_{si}}{\partial R} + \frac{\partial^2 \theta_{si}}{\partial Z^2} \right) \tag{2}$$

$$\frac{\partial \theta_f}{\partial \mathrm{Fo}} = \frac{\partial^2 \theta_f}{\partial R^2} + \frac{1}{R} \frac{\partial \theta_f}{\partial R} + \frac{\partial^2 \theta_f}{\partial Z^2} \tag{3}$$

where θ, R, and Z are the dimensionless temperature and radial and longitudinal coordinates, respectively. Fo is the Fourier number. These are defined as

$$\theta = \frac{T - T_0}{q_v r_i^2 / \lambda}, \qquad \mathrm{Fo} = \frac{\alpha t}{r_i^2}, \qquad R = \frac{r}{r_i}, \qquad Z = \frac{z}{r_i} \tag{4}$$

The parameters R_{c1}, R_{d1}, etc., and those appearing in the boundary conditions are the thermal conductivity and thermal diffusivity ratios of each layer, defined as

$$R_{c1} = \frac{\lambda}{\lambda_{sh}}, \qquad R_{c2} = \frac{\lambda_{si}}{\lambda_{sh}}, \qquad R_{c3} = \frac{\lambda}{\lambda_{si}}, \qquad R_{d1} = \frac{\alpha}{\alpha_{sh}}, \qquad R_{d2} = \frac{\alpha}{\alpha_{si}} \tag{5}$$

where λ and α are the thermal conductivity and the thermal diffusivity, respectively, and where the subscripts sh and si indicate short hot wire and insulating material, respectively.

These equations are solved by a finite difference method with an implicit subsequent substitution scheme, under relevant initial and boundary conditions including the continuity conditions for temperature and heat flux at the interfaces between the hot wire and the coating layer and between the coating layer and the liquid layer. A nonuniform grid arrangement is used and the node numbers are 101 and 201 in the Z and R directions, respectively.

The numerical analysis yields the dimensionless volume-averaged hot-wire temperature θ_v as a function of the dimensionless heating time Fo. The numerical error is confirmed to be within 0.2% for the range of Fo = 5 to 100, when the solution corresponding to an infinite length wire is compared with that obtained analytically. The effect of the boundary conditions at $R = R_o$ is also examined to estimate the minimum radius of the vessel to achieve accurate measurement. The results indicate that if $R_o > 50$, the time variation of θ_v becomes independent of the thermal boundary condition for $R = R_o$ (adiabatic or isothermal). This fact indicates that a very small amount of sample liquid is required in the present method.

The detailed effects of aspect ratios $L(l/r_i)$, insulating layer thickness δ, and the parameters R_{c1} and R_{d1} on the wire temperature θ_v are given in Ref. 5. These results are summarized as follows: (a) as the aspect ratio L decreases, the slope in the relation, θ_v vs. ln Fo, decreases because the conductive heat loss to the lead wire takes up a large fraction of the heat generated in the hot wire; (b) with the increase in δ, the temperature rise becomes smaller but the slope remains constant; and (c) as R_{c1} decreases, θ_v decreases because the relative heat loss from the wire edges to the supports increases with the decrease in liquid thermal conductivity. Since the relation between θ_v and ln Fo depends on the liquid thermal properties, numerical calculations with wide ranges of parameters must be done before applying this method to unknown samples. Further, in this method the thermal conductivity and thermal diffusivity of fluid should be determined simultaneously. This is the largest difference from the conventional hot-wire method, which is based on a single working equation.

3. PRINCIPLE OF MEASUREMENTS

Based on the numerical results, the following procedure was proposed to determine simultaneously the thermal conductivity and thermal diffusivity of a liquid. As described in Ref. 5, the dimensionless temperature increases linearly from Fo = 5 to, at least, Fo = 150. The real time corresponding to Fo = 150 ranges from 2 to 4 s, depending on the kind of liquid. Then, the numerical results in this time range are approximated by a linear equation, Eq. (6), and the coefficients A and B are determined by the least-squares method.

$$\theta_v = A \ln \mathrm{Fo} + B \tag{6}$$

The measured temperature rise of a wire could also be approximated by a linear equation with coefficients a and b in the above time range as

$$T_v = a \ln t + b \tag{7}$$

where T_v is the wire temperature rise based on the T_o. Equation (6) is dimensionalized as

$$T_v = \frac{q_v r_i^2}{\lambda} A \ln t + \frac{q_v r_i^2}{\lambda}\left(A \ln \frac{\alpha}{r_i^2} + B\right) \tag{8}$$

Comparing the corresponding coefficients of Eqs. (7) and (8), the thermal conductivity and thermal diffusivity of a liquid are expressed as functions of these coefficients by

$$\lambda = q_v r_i^2 \frac{A}{a} = \frac{VI}{2\pi l}\frac{A}{a} \tag{9}$$

$$\alpha = r_i^2 \exp\left(\frac{b}{a} - \frac{B}{A}\right) \tag{10}$$

where V and I are the voltage and current supplied to the wire. Equations (9) and (10) are similar to those obtained for the conventional transient hot-wire method [7], except that the A and B are changed somewhat in relation to the aspect ratio L, parameters R_{c1} and R_{d1}, etc., so that an iterative process is required to evaluate thermal properties accurately.

From Eqs. (9) and (10) the relative errors of the thermal conductivity and thermal diffusivity are estimated as

$$\frac{\delta\lambda}{\lambda} = \left\{\left(\frac{\delta V}{V}\right)^2 + \left(\frac{\delta I}{I}\right)^2 + \left(\frac{\delta l}{l}\right)^2 + \left(\frac{\delta A}{A}\right)^2 + \left(\frac{\delta a}{a}\right)^2\right\}^{1/2} \tag{11}$$

$$\frac{\delta\alpha}{\alpha} = \left[\left(\frac{2\delta r_i}{r_i}\right)^2 + \left\{\delta\left(\frac{B}{A}\right)\right\}^2 + \left\{\delta\left(\frac{b}{a}\right)\right\}^2\right]^{1/2} \tag{12}$$

The magnitudes of the main factors in Eqs. (11) and (12) are estimated as follows. The length and radius of the hot wire are measured with a microcathetometer and microscope, and both $\delta l/l$ and $\delta r_i/r_i$ are accurate to 1%. The possible error in the slope of the temperature against $\ln t$ includes the uncertainties induced by electrical noise and the timing of the voltage measurements. The maximum deviation of the temperature measurement from Eq. (7) is less than 0.2%. The values of $\delta a/a$ and $\delta(b/a)$ are around 0.01 and 0.04, respectively. From numerical solutions, $\delta A/A$ is found to be 0.002 and $\delta(B/A)$ is 0.003. The voltage and current through the wire are measured with digital multimeters and the values of $\delta V/V$ and $\delta I/I$ in the measurement are less than 10^{-4}. The total errors of this method are estimated to be 2 and 5% for thermal conductivity and thermal diffusivity,

respectively, when the thickness and thermal properties of the insulating film are precisely known.

4. MEASUREMENTS

4.1. Hot-Wire Cell

Figure 2 shows the transient short-hot-wire cell used in this study. A short platinum wire 9.2 mm in length and 97 μm in diameter (1) is welded at both ends to platinum lead wires of 1.5 mm in diameter (3) which is supported with a ceramic circular plate (2) and connected with voltage (5) and current (6) platinum lead wires 0.5 mm in diameter. The ceramic plate is fixed with a stainless-steel rod which can move up and down. A pure gold crucible (4) 50 mm in diameter and 120 cm^3 in volume is heated with an electric furnace (8) which is covered with a thermal insulator (9) on the outside. The temperatures at the outside of the crucible wall are measured with thermocouples (7) to provide a feedback signal for the temperature controller. The measurements are made at different temperature levels and atmospheric pressure.

The platinum hot wire is annealed at 800°C for a few hours, and the temperature coefficient of its electrical resistance β is determined through a calibration for the temperature range from 20 to 800°C. This wire is cut and welded to the platinum lead terminals. The probe has to be carefully cleaned with ultrasonic cleaner before it is fixed in the chamber of the sputtering apparatus. Figure 3 shows a schematic of the rotating part of the

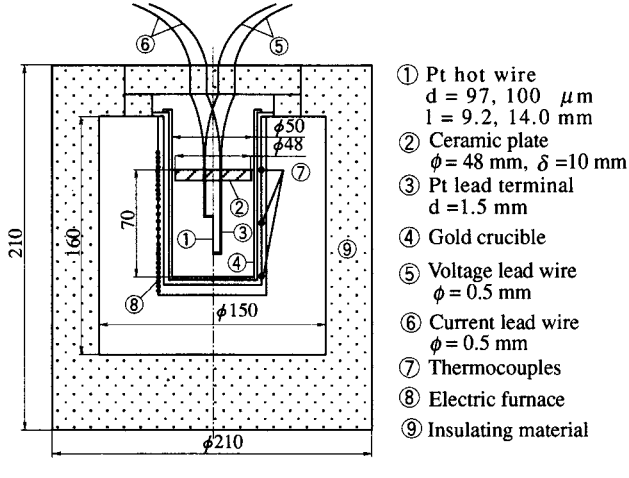

Fig. 2. Schematic of the experimental setup.

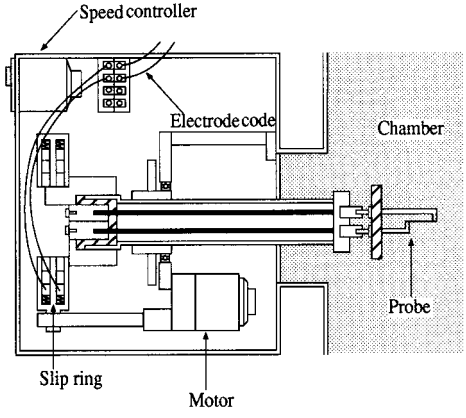

Fig. 3. Rotating part of the sputtering apparatus.

sputtering apparatus. The probe is mounted on the right top side and rotates at a constant speed during the coating process so that the present sputtering apparatus can provide a uniform thin film on the cylindrical wire. In the present case, high-purity (99.99%) Al_2O_3 is used as the coating material. The output of sputtering power is controlled at 100 W. The chamber gas pressure is 0.22 Pa. The flow rates of argon and oxygen gases are controlled at 10 and 5 $cm^3 \cdot min^{-1}$, respectively. The sputtering time is 6.4 h for a film thickness of 2 μm. The coated probe is again calibrated to determine its total resistance including the lead terminals Rt_o at 0°C, under the assumption that the coefficient of the lead wire is the same as β. When the probe is immersed in a liquid with uniform temperature, the hot-wire temperature is obtained as

$$T_v = \frac{1}{\beta}\left(\frac{Ri}{Rt_0} - 1\right) \tag{13}$$

where Ri is the measured resistance of the probe. On the other hand, when the probe is heated, the wire temperature rises but the lead terminal temperature remains at the initial temperature because of its large heat capacity. Therefore, the hot-wire temperature is estimated as

$$T_v = \frac{1}{\beta}\left(\frac{Rt(t) - \varepsilon Ri}{(1-\varepsilon)\, Rt_0} - 1\right) \tag{14}$$

where ε is the resistance ratio of the lead terminals and the entire probe and is about 0.075 for the present probes.

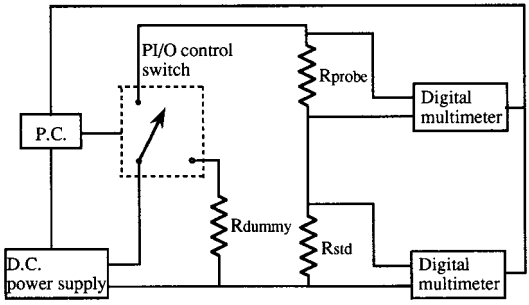

Fig. 4. Schematic of the measurement system.

4.2. Measurement System

The measuring system is shown schematically in Fig. 4. It is composed of a dc power supply and voltage and current measuring and control systems, that is, digital multimeter, personal computer, and PI/O controller. The power supply can generate a maximum constant current of 1 A with 1.5-mA resolution. Two DMs are the same type and have a 7.5-digit accuracy at a sampling rate of 20 per s. The PC controls both switching and logging of data.

The data acquisition procedure is almost the same as with the conventional hot-wire method. After the liquid temperature becomes uniform and constant, a small current, such as 15 mA, is supplied to the probe for 3 s to measure the initial liquid temperature. Then the switch is turned on to the dummy circuit, having the same resistance as the main circuit including the probe, and a heating current of 0.3 to 0.5 A is supplied. After 1 s, when the current becomes stable, the switch is again closed to the main circuit to begin heating the hot wire. In this process, the current and voltage are measured 20 times per s. These measurements are carried out automatically using a sequential program and GP-IB controlled by a personal computer.

5. RESULTS AND DISCUSSION

At first, the characteristics of the short-hot-wire probe are examined using pure water and toluene as standard liquids with known thermal conductivity and thermal diffusivity. The temperature evolutions for these liquids are compared with corresponding numerical results, and the evaluated thermal conductivity and thermal diffusivity are compared with reference values [6]. Then, the effective hot-wire length and diameter and the resistance ratio of the lead terminals and the entire probe are determined.

The length differs by, at most, 3% from that measured with a microcathetometer. The reason for the difference is attributed mainly to an uncertainty of accurate welding positions on the lead terminals. The thermal conductivity and thermal diffusivity of these standard liquids have been measured under normal gravity conditions, because the effect of natural convection will not appear, at least in the range $Fo < 200$ [8, 9]. The reproducibility of the hot-wire temperature rise is examined for water, and it is confirmed that the differences among the repeated data are within 0.01°C, if we allow more than 60 min between successive measurements.

Table I shows the measured thermal conductivity and thermal diffusivity of $NaNO_3$, Li_2CO_3/K_2CO_3, and Li_2CO_3/Na_2CO_3, respectively. These data are the average values of three measurements at the same temperature. The tested samples were supplied by Wako Pure Chemical Industries Ltd. and had a stated purity in excess of 99.95%. Table I also shows the reproducibility for the present measurements of the thermal conductivity and thermal diffusivity.

Figures 5 and 6 show the measured thermal conductivity and thermal diffusivity of $NaNO_3$, respectively. The dashed lines show the results obtained by Kobayashi et al. [10]; the solid line in Fig. 5 shows the recommended correlation proposed by Kitade *et al* [11]; the open circles

Table I. Measured Thermal Conductivity and Thermal Diffusivity

Substance	Temperature T (°C)	Measured λ ($W \cdot m^{-1} \cdot K^{-1}$)	Measured α ($m^2 \cdot s^{-1}$)	Reproducibility λ and α ($\pm$%)
$NaNO_3$	330.8	0.557	1.59E-7	0.7, 1.9
	350.8	0.573	1.88E-7	1.0, 4.8
	390.4	0.588	2.00E-7	1.0, 1.5
Li_2CO_3–K_2CO_3 (70/30 mol%)	547.6	0.729	0.60E-7	0.4, 10.0
	589.8	0.697	0.46E-7	1.7, 17.4
	610.2	0.691	0.46E-7	2.7, 15.2
	649.0	0.829	0.98E-7	0.8, 12.2
Li_2CO_3–Na_2CO_3 (53/47 mol%)	564.3	0.892	1.16E-7	1.6, 4.3
	587.1	0.824	0.76E-7	1.8, 7.9
	592.9	0.848	2.00E-7	1.3, 6.0
	611.4	0.923	1.47E-7	0.8, 7.5
	637.1	0.875	0.93E-7	0.3, 4.3
	650.8	0.877	1.19E-7	0.3, 6.7
	651.2	0.885	1.23E-7	1.9, 2.4
	685.3	0.887	0.98E-7	0.2, 1.0
	694.5	0.875	0.83E-7	1.6, 13.3

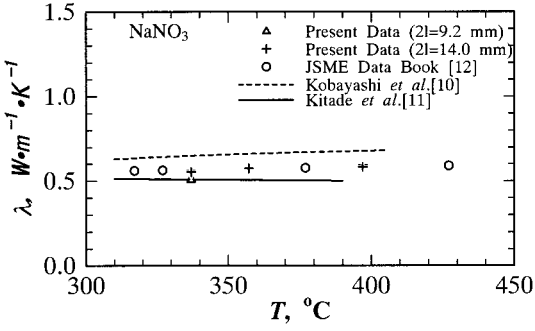

Fig. 5. Measured thermal conductivity for $NaNO_3$.

indicate the reference values of the JSME Data Book [12]; and the symbols △ and + indicate the present values obtained with two different probes. By comparing the present results with the reference values of the JSME Data Book, the errors for the thermal conductivity and thermal diffusivity are within ±3 and ±20%, respectively.

Figures 7 and 8 show the thermal conductivity and thermal diffusivity of Li_2CO_3/K_2CO_3, respectively. Figures 9 and 10 show those of Li_2CO_3/Na_2CO_3. The dashed lines are obtained with a linear least-squares method for the present data; the solid lines show the results obtained by Araki et al. [13]; the symbol □ indicates the results obtained by Otsubo et al. [14]; and the other symbols, +, △, ○, and ◎, indicate the present results. By comparing the present results with the data of Araki et al., the thermal conductivity of Li_2CO_3/K_2CO_3, as shown in Fig.7, shows good aggreement, but the thermal conductivity of Li_2CO_3/Na_2CO_3 in Fig. 9 shows a different tendency to temperature change. Further, comparing with

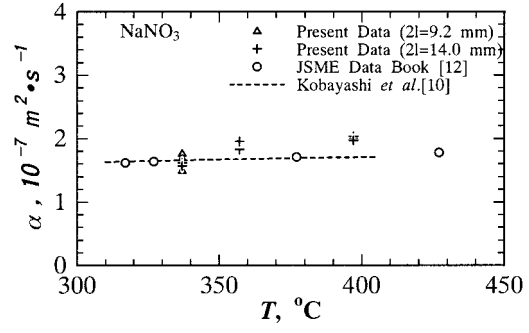

Fig. 6. Measured thermal diffusivity for $NaNO_3$.

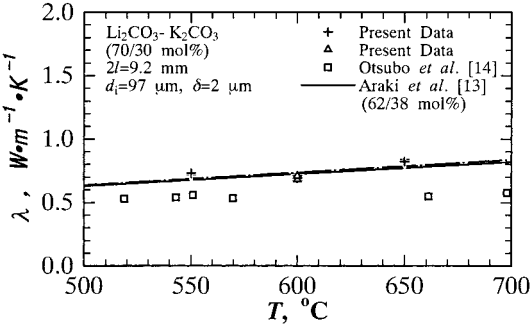

Fig. 7. Measured thermal conductivity for Li_2CO_3/K_2CO_3.

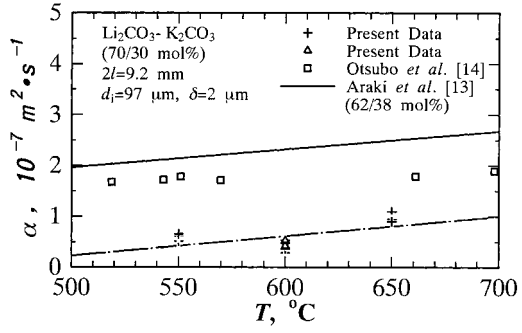

Fig. 8. Measured thermal diffusivity for Li_2CO_3/K_2CO_3.

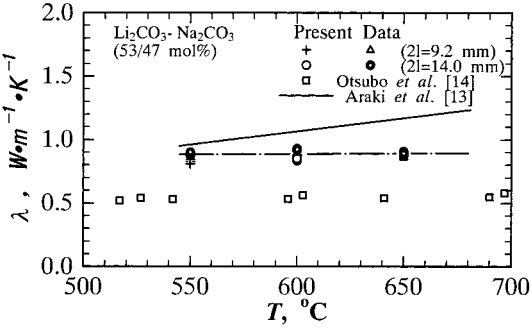

Fig. 9. Measured thermal conductivity for Li_2CO_3/Na_2CO_3.

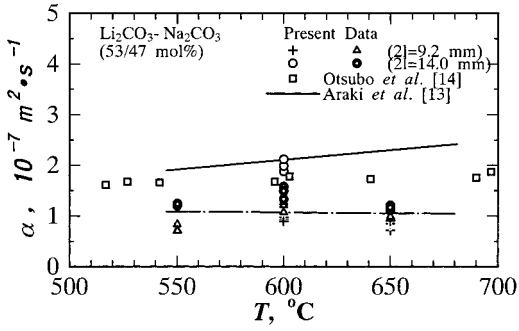

Fig. 10. Measured thermal diffusivity for Li_2CO_3/Na_2CO_3.

the data of Otsubo et al., both the thermal conductivity and thermal diffusivity show large differences between the results.

Figure 11 shows the effect of an uncertainty of thermal diffusivity on estimating the thermal conductivity. It is found from this figure that the gradient of masterplot A is changed within 5% even for a 50% change of the thermal diffusivity ratio R_{d1} for the present case of $R_{d1} = 0.003$. Therefore, the present method has, at least, reasonable accuracy for measuring thermal conductivity.

6. CONCLUSIONS

The main conclusions are as follows.

(1) The transient short-hot-wire method has been successfully used to measure the thermal conductivity and thermal diffusivity of

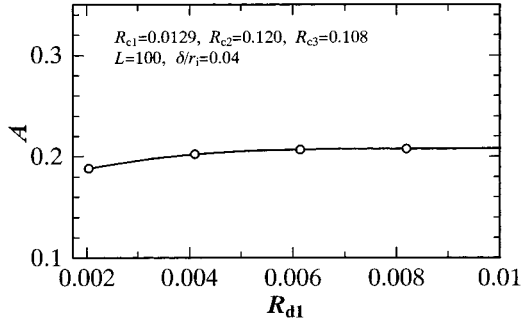

Fig. 11. Effect of uncertainty of thermal diffusivity on thermal conductivity.

molten salts simultaneously when the probe was coated with pure Al_2O_3 as an insulating film. The method can determine the thermal conductivity and thermal diffusivity for molten nitrate within errors of 3 and 20%, respectively. Also the thermal conductivity of molten carbonates can be measured within an error of 5%, although the thermal diffusivity can be measured within an error of 50%.

(2) Though the accuracy is not as high as that of the conventional transient hot-wire measurement, the present method is much more convenient and has sufficient accuracy to yield reasonable results for new liquids. The method, therefore, will be applied for measuring these properties of electrically conducting liquids, when the probe is adequately coated with insulating and anti-corrosive materials.

(3) The measurement accuracy is expected to be improved after the effects of film thickness and its properties are studied and considered in detail.

ACKNOWLEDGMENTS

This work is supported partly by the Grant-in-Aid for Scientific Research B0755538 from the Ministry of Education, Science, Sports and Culture of Japan. The authors also express their thanks to Mr. R. Miyazaki, Mr. Z. Qi, Mr. K. Hamano, and Dr. Y. Akiyama at the Institute of Advanced Material Study, Kyushu University for their assistance.

REFERENCES

1. H. Shibata, H. Ohta, and Y. Waseda, *Mater. Trans. JIM* **32**:837 (1991).
2. M. J. Assael, C. A. Nieto de Castro, H. M. Roder, and W. A. Wakeham, in *Experimental Thermodynamics, Vol. III. Measurement of the Transport Properties of Fluid*, W. A. Wakeham, A. Nagashima, and J. V. Sengers, eds. (Blackwell Scientific, Oxford, 1991), Chap. 7.
3. Y. Nagasaka and A. Nagashima, *Trans. JSME* **47**:1323 (1981).
4. X. Zhang, T. Tomimura, and M. Fujii, in *Proc. 14th Japan Symp. Thermophys. Prop.* (Jpn. Soc. Thermophys. Prop., 1993), pp. 23–26.
5. M. Fujii, X. Zhang, N. Imaishi, S. Fujiwara, and T. Sakamoto, *Int. J. Thermophys.* **18**:327 (1997).
6. C. A. Nieto de Castro, S. F. Y. Li, A. Nagashima, R. D. Trengove, and W. A. Wakeham, *J. Phys. Chem. Ref. Data* **15**:1073 (1986).
7. N. Nagasaka and A. Nagashima, *Rev. Sci. Instrum.* **52**:229 (1981).
8. S. T. Ro, J. H. Lee, and J. Y. Yoo, in *Thermal Conductivity 21* (Plenum Press, New York, 1990), pp. 151–164.
9. X. Zhang, S. Fujiwara, Z. Qi, and M. Fujii, *J. Jpn. Soc. Micrograv. Appl.* **16**(2):129 (1999).

10. K. Kobayashi, N. Araki, and Y. Iida, in *Proc. 7th Int. Heat Transfer Conf., Vol. 6* (1982), pp. 467–472.
11. S. Kitade, Y. Kobayashi, Y. Nagasaka, and A. Nagashima, *High Temp.-High Press.* **21**:219 (1989).
12. *JSME Data Book: Heat Transfer*, 4th ed. (1986).
13. N. Araki, M. Matsuura, and T. Hirata, in *Proc. 8th Japan Symp. Thermophys. Prop.* (Jpn. Soc. Thermophys. Prop., 1987), pp. 1–4.
14. S. Otsubo, Y. Nagasaka, and A. Nagashima, *Trans. JSME* **61**:806 (1998).